

Received: 2020.12.01
Accepted: 2021.01.29
Available online: 2021.02.05
Published: 2021.04.01

Effect of Fluorofenidone Against Paraquat-Induced Pulmonary Fibrosis Based on Metabolomics and Network Pharmacology

Authors' Contribution:
Study Design A
Data Collection B
Statistical Analysis C
Data Interpretation D
Manuscript Preparation E
Literature Search F
Funds Collection G

AE 1 **Feiya Jiang**
B 1 **Tongtong Wang**
D 2 **Sha Li**
C 3 **Yu Jiang**
F 4 **Zhuo Chen**
AG 1 **Wen Liua**

1 Department of Pharmacy, The First Hospital Affiliated with Hunan Normal University, Changsha, Hunan, P.R. China
2 Department of Pharmacy, Changsha Stomatological Hospital, Changsha, Hunan, P.R. China
3 Emergency Medical Research Institute, Hunan Provincial People's Hospital, Changsha, Hunan, P.R. China
4 Xiangya College of Pharmacy, Central South University, Changsha, Hunan, P.R. China

Corresponding Author: Wen Liu, e-mail: liuwen@hunnu.edu.cn

Source of support: This work was supported by the Scientific Research Project of Hunan Provincial Commission of Health and Family Planning (No. B2017076), a research project with the Changsha Science and Technology Department (No. kq1901051) and the Foundation of Hunan Provincial Key Laboratory of Emergency and Critical Care Metabonomics

Background: Fluorofenidone (AKF-PD) is an anti-fibrotic small-molecule compound. Its mechanism of action on paraquat (PQ)-induced pulmonary fibrosis is still unclear.





Material/Methods: Forty-eight SD rats were divided into 4 groups: control group, PQ group, PQ+AKF-PD group, and AKF-PD group. The pathological changes of lung tissues were observed by Masson and HE staining. The UPLC-QTOF-MS analysis was performed to detect the differences in metabolites among groups, then the possible mechanisms of the anti-pulmonary fibrosis effects of fluorofenidone were further revealed by network pharmacology analysis. Biological methods were used to verify the results of the network pharmacology analysis.

Results: The results showed that fluorofenidone treatment significantly alleviated paraquat-induced pulmonary fibrosis. Metabolomics analysis showed that 18 metabolites were disordered in the serum of paraquat-poisoned rats, of which 13 were restored following fluorofenidone treatment. Network pharmacology analysis showed that the drug screened a total of 12 targets and mainly involved multiple signaling pathways and metabolic pathways to jointly exert anti-pulmonary fibrosis effects. Autophagy is the main pathway of fluorofenidone in treatment pulmonary fibrosis. The western blot results showed that fluorofenidone upregulated the expression of LC3-II/I and E-cadherin, and downregulated the expression of p62, α -SMA, and TGF- β 1, which validated that fluorofenidone could inhibit the development of paraquat-induced pulmonary fibrosis by increasing autophagy.

Conclusions: In conclusion, metabolomics combined with network pharmacology research strategy revealed that fluorofenidone has a multi-target and multi-path mechanism of action in the treatment of pulmonary fibrosis.

Keywords: **Idiopathic Pulmonary Fibrosis • Metabolic Networks and Pathways • Metabolomics • Paraquat • Protein Interaction Maps**

Full-text PDF: <https://www.medscimonit.com/abstract/index/idArt/930166>

 4158  1  10  56



Background

Paraquat is a non-selective herbicide widely used in developing countries. It is highly toxic to humans and animals, and the lung is its main target organ [1]. Paraquat poisoning results in the development of acute multiple-organ failure followed by pulmonary fibrosis and death from respiratory failure. Pulmonary fibrosis is a typical feature of paraquat poisoning, which is characterized by progressive dyspnea, pulmonary ventilation dysfunction, inflammatory response, and destruction of lung parenchymal structure [2,3]. Guidelines for the treatment of pulmonary fibrosis have not been fully developed, and current treatment methods include drug therapy, mechanical ventilation, and lung transplantation, but the therapeutic effect is not satisfactory [4,5]. Therefore, it is urgent to develop more effective therapeutic agents for pulmonary fibrosis.

The United States Food and Drug Administration recently approved pirfenidone as a treatment for idiopathic pulmonary fibrosis [6]. Pirfenidone (PFD) is a broad-spectrum oral anti-fibrotic drug originally used as an anti-inflammatory agent, and it can reduce the expression of transforming growth factor β 1 (TGF- β 1), α -smooth muscle actin (α -SMA), type I collagen, and tumor necrosis factor (TNF) [7]. Furthermore, pirfenidone has been shown to exert antioxidant activity in vivo and to reduce pulmonary fibrosis and mortality in paraquat-exposed rats [8,9]. Fluorofenidone is a drug that is similar to pirfenidone, a small-molecule compound indicated for anti-fibrotic activity, where a fluorine atom replaces the hydrogen atom in the benzene ring. This structural modification can improve the stability and biological activity of compounds [10]. Previous studies have shown that fluorofenidone has a broad and confirmed anti-organ-fibrotic effect, including anti-liver fibrosis, anti-renal fibrosis, and anti-cardiac fibrosis [11-13]. The mechanism of fluorofenidone against organ fibrosis involves reducing inflammation, anti-oxidative stress, inhibiting cell proliferation and activation, and promoting extracellular matrix (ECM) degradation [14-16]. It was reported that fluorofenidone effectively inhibited the activation of human lung fibroblasts induced by transforming growth factor β 1 and reduce the expression of type I collagen and fibronectin [17]. Moreover, fluorofenidone was shown to reduce the degree of bleomycin-induced pulmonary fibrosis in mice and the expression of type I collagen and fibronectin in lung tissues, and its therapeutic effect is estimated to be equivalent to that of pirfenidone [18]. More importantly, the half-life of oral fluorofenidone is twice that of pirfenidone [19], suggesting that fluorofenidone is more appropriate for the long-term treatment of pulmonary fibrosis. However, the effect and mechanism of fluorofenidone in treating paraquat-induced pulmonary fibrosis are still unclear. Therefore, we aimed to investigate the metabolic profiles and the underlying mechanisms of fluorofenidone in paraquat-induced pulmonary fibrosis and to provide a theoretical basis for the clinical application of fluorofenidone.

Metabolomics is a high-throughput method for identifying and quantifying small components of the metabolome (molecular weight <1500 Da) [20]. Analyzing the changes of metabolites after treatment with medicine can reveal their underlying efficacy and mechanisms of action [21]. Network pharmacology is a new research field based on the theory of system biology, which analyzes the networks of a biological system and selects specific signal nodes to carry out multi-target drug molecular design [22]. Network pharmacology emphasizes the multi-channel regulation of signaling pathways, improving the therapeutic effect of drugs, and reducing the adverse effects, so as to improve the success rate of clinical trials of new drugs. In this study, metabolomics and network pharmacology methods were integrated to explore the potential mechanism of fluorofenidone against paraquat-induced pulmonary fibrosis.

Material and Methods

Reagents

Fluorofenidone (Lot No. 180212) was synthesized by the School of Pharmaceutical Sciences, Central South University. PQ was purchased from Syngenta Nantong Crop Protection Co., Ltd. (Nantong, China). Formic acid (FA) (HPLC grade) was purchased from Aladdin Industrial Co., Ltd. (Shanghai, China). Methanol (HPLC grade) and acetonitrile (HPLC grade) were purchased from Merck (Darmstadt, Germany). LC3, p62 rabbit antibody was from Abcam, USA and the BCA protein assay kit was from Thermo Scientific, USA.

Animals and Groups

Forty-eight Sprague-Dawley (SD) male rats weighing 200-220 g were purchased from Hunan Slake Jingda Experimental Animal Co., Ltd. (license: SCKK (Xiang) 2016-0002). These rats were placed in an environment of 22.2°C, 50-60% humidity, with free access to food and water. All the experiments were approved by the Animal Laboratory (Changsha) of Hunan Provincial People's Hospital. After 3 days of acclimation, the rats were divided into 4 groups according to the random number table: control group, PQ group, AKF-PD group, and PQ+AKF-PD group. The control group was given 1 ml normal saline by gavage every day; the PQ group and the PQ+AKF-PD group were administered 40 mg/kg PQ at one time. Two hours later, the AKF-PD group and the PQ+AKF-PD group were administered fluorofenidone daily (500 mg/kg) [23]. Meanwhile, the control group and PQ group were injected with the same amount of saline in the tail vein. All treatments were administered continuously for 14 days, and the rats were anesthetized with 3% sodium pentobarbital and euthanized by neck dislocation. The lung tissues and plasma were collected from each group and stored at -80°C for future study. The experimental animal methods all conformed to animal ethics standards.

Oxidative Stress and Collagen Content

To analyze the level of oxidative stress and the degree of fibrosis in the lung tissue, lung tissue was collected from each group and then weighed, diluted with 10% physiological saline, and centrifuged at 3500 rpm for 10 min, and then were assessed with a microplate reader and automatic biochemical detector. After that, the content of malondialdehyde (MDA) was determined by thiobarbituric acid colorimetry. The enzyme activity of superoxide dismutase (SOD) and the content of hydroxyproline (HYP) were determined according to the instructions of the kit.

Histopathology

The lung tissue was fixed, dehydrated, transparentized, and embedded in paraffin. The paraffin section was dewaxed twice with xylene and then hydrated in an ethanol gradient (100%, 95%, 80%, 70%). HE staining and Masson's trichrome staining was performed according to the instructions of the reagent. The sections were observed and photographed under a microscope with 200× magnification. The degree of pulmonary fibrosis and alveolitis were evaluated according to the method described by Szapiel et al [24].

Sample Preparation

The plasma samples (200 µL) from each group were transferred to the refrigerator and thawed at 4°C. Then, 600 µL methanol was added to the plasma and centrifuged at 12 000 rpm for 15 min to separate the protein. Subsequently, 600 µL supernatant was dried under vacuum at room temperature, and a 200-µL acetonitrile: water (1: 1) mixture was added, then centrifuged at 12000 rpm for 15 min at low temperature. Finally, 10 µL supernatant was injected into a UPLC-QTOF-MS system for analysis.

UPLC-QTOF-MS Analysis

The metabolites in plasma were separated by ultra-high-performance liquid chromatography (UPLC), and 10 µL of each sample was injected into an Acclaim TM RSL120-C18 column (100×2.1 mm, 2.2 µm, 120A, Thermo Fisher Scientific, USA) at a flow rate of 0.2 mL/min, and the column temperature was maintained at 30°C. The mobile phase was composed of 0.1% formic acid (A) and acetonitrile (B). The optimized UHPLC elution conditions were set at: 2% B, 0-2 min; 2-50% B, 2-12 min; 50-90% B, 12-20 min; 90% B, 20-30 min; 2% B, 30.1 min, and 2% B at 30.1-35 min to re-equilibrate the column.

The electrospray ionization source (ESI) was operated in both positive and negative ion modes. The mass spectrometric (MS) conditions used were as follows: ion injection voltage was set

at 4500 V; endplate offset voltage was 500 V; dry gas, Nitrogen; capillary temperature, 200°C; gas flow, 8.0 L/min; MS/MS Collision Energy was set from 20 to 50 eV; mass-to-charge ratio (M/Z) range 20-1000; scanning time 8.00 Hz, and the inter-scan delay 0.1 s. To avoid possible contamination and to keep the signal stable and determine the exact molecular weight, each sample was calibrated with a solution of sodium formate prior to injection for optimal accuracy and reproducibility.

Data Pre-processing and Statistical Analysis

The data detected by the UPLC-QTOF-MS were imported into Metascape 3.0 (Bruker Corporation) to detect and align the peak values of all samples. After being identified and aligned, we normalized the intensity of each ion with the total ion strength in each chromatogram. We identified the compounds by using the standard sample database, the downloaded HMDB database, and the online search database provided by Brook. Finally, the three-dimensional matrix information included retention time (RT), mass-charge ratio (m/z), ionic strength information (variable), and compound names. After the extracted data were modified in accordance with the import format and information integrity principles, data were imported into the multivariate statistical software SIMCA (version 14.1, Umetrics, Umea, Sweden) for principal component analysis, and then subjected to UV pre-processing for partial deviation. Partial least-squares discriminant analysis (PLS-DA) was used to screen potential biomarkers. To further screen out the significant variables among different groups, the metabolic information data detected by the instrument were imported into SPSS 22.0 software (IBM, USA) for one-way ANOVA. Finally, the variables with a variable importance plot (VIP) >1 in the PLS-DA model and p<0.05 in the *t* test were considered as potential biomarkers. MetaboAnalyst (<http://www.metaboanalyst.ca>) and KEGG (<https://www.kegg.jp>) were used for the enrichment analysis and metabolic pathways analysis.

Network Pharmacology Analysis

Drugs exert effects by binding their molecule to a specific target and regulating the biological activity or transcription level of the target. Therefore, it is of great significance to investigate the compound-target interaction to elucidate its mechanism of action.

The 3D structure of fluorofenidone was download from the PubChem database (<https://pubchem.ncbi.nlm.nih.gov/>), and then the relevant therapeutic targets were obtained from the SwissTargetPrediction database (<http://www.swisstargetprediction.ch/index.php>). We set the search term to "pulmonary fibrosis" in GeneCards (<https://geneacart.genecards.org/>) and OMIM (<https://www.omim.org/>) databases to download the related disease genes. Finally, the results from the 2 databases

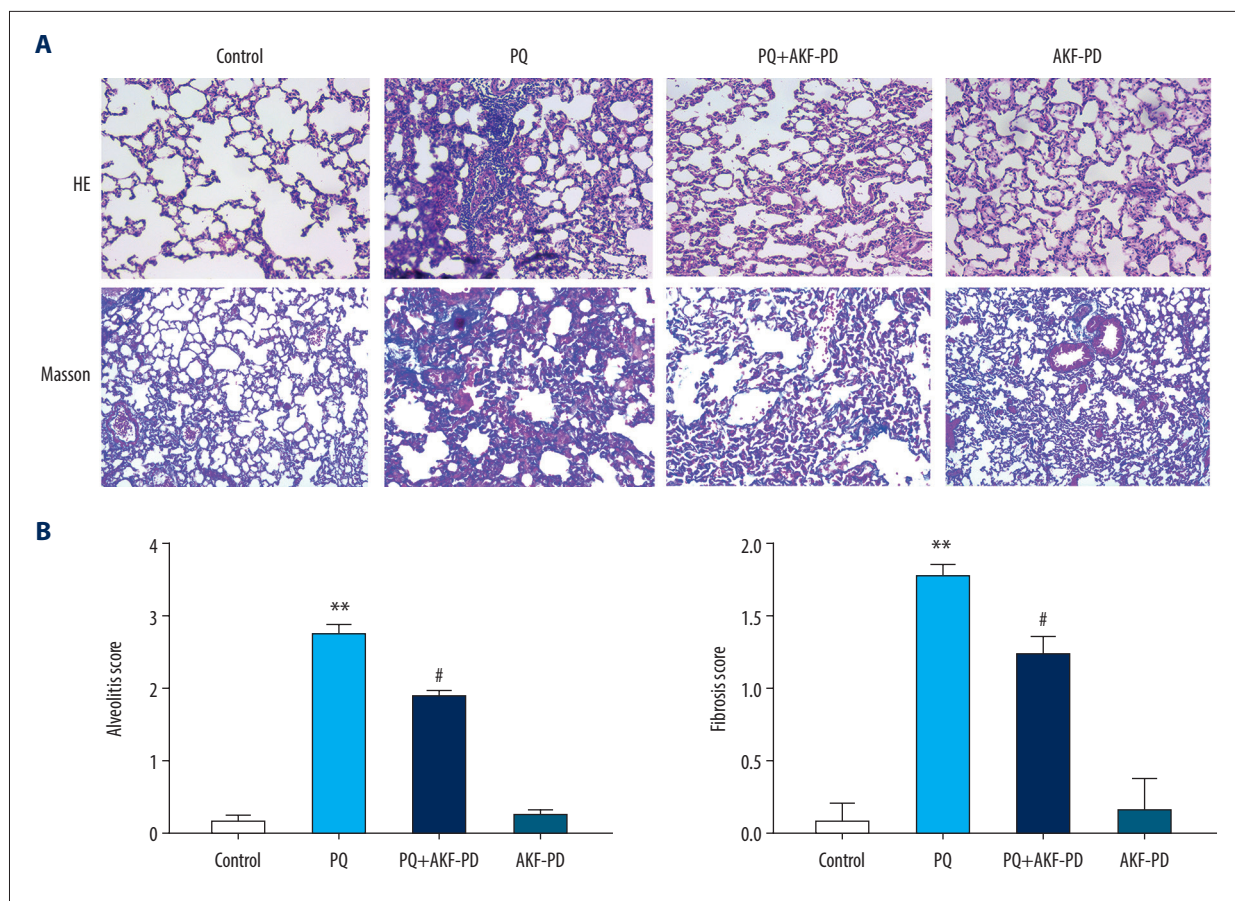


Figure 1. Pathological changes in rat lung tissue were observed under a light microscope. **(A)** Representative images of H&E and Masson's-stained lung sections from the 4 experimental groups (magnification: 200 \times); **(B)** Statistical analysis of the levels of alveolitis and pulmonary fibrosis scores. ** $P < 0.01$ vs the control group; # $P < 0.05$ vs the PQ group. PQ – paraquat; AKF-PD – fluorofenidone.

were summarized to obtain the disease genes related to pulmonary fibrosis. Subsequently, we organized the drug targets and disease targets, imported the data into R \times 64 4.0.2, drew a Venn diagram (Venn) using Bioconductor databases (<http://www.bioconductor.org/>), and obtained the intersection genes. Cytoscape-3.7.0 software was used to construct the “Fluorofenidone-target-pulmonary fibrosis” disease network diagram, in which the attributes of the nodes include drugs, co-acting targets, and diseases. To assess the role of target proteins of the compound in signaling pathways, R-Studio software was used to perform Gene Ontology (GO) enrichment analysis and Kyoto Encyclopedia of Genes and Genomes (KEGG) metabolic pathway enrichment analysis. The significance threshold was set as $P < 0.05$, and the main biological process and signal pathway of fluorofenidone in the treatment of pulmonary fibrosis were obtained.

Western Blot Analysis was Performed to Detect the Expression of Autophagy-related Proteins

The lung tissues were homogenized in a lysis buffer. A protein assay kit (BCA; Thermo Scientific, USA) was used to measure the total protein in samples. The equal total protein was separated in SDS-PAGE, then transferred to a polyvinyl alcohol membrane, and sealed with milk at room temperature for 1 h. The membrane was incubated overnight with a primary antibody at 4°C. As primary antibodies, we used rabbit monoclonal antibody against TGF- β 1 (1: 2000), α -SMA (1: 2000), E-cadherin (1: 1000), mTOR (1: 3000), LC3 (1: 4000), p62 (1: 2000), and β -actin (1: 2000), all purchased from Abcam. β -actin was used as a loading control to normalize the data. The membrane was washed with TBST 3 times and incubated with horseradish peroxidase-linked anti-rabbit antibody (1: 4000) at room temperature for 1 h. The ECL kit was used for luminescent development, a chemiluminescence instrument was used to scan the strip, and Image Lab software was used to analyze the gray value of the strip. Protein expression was normalized to β -actin.

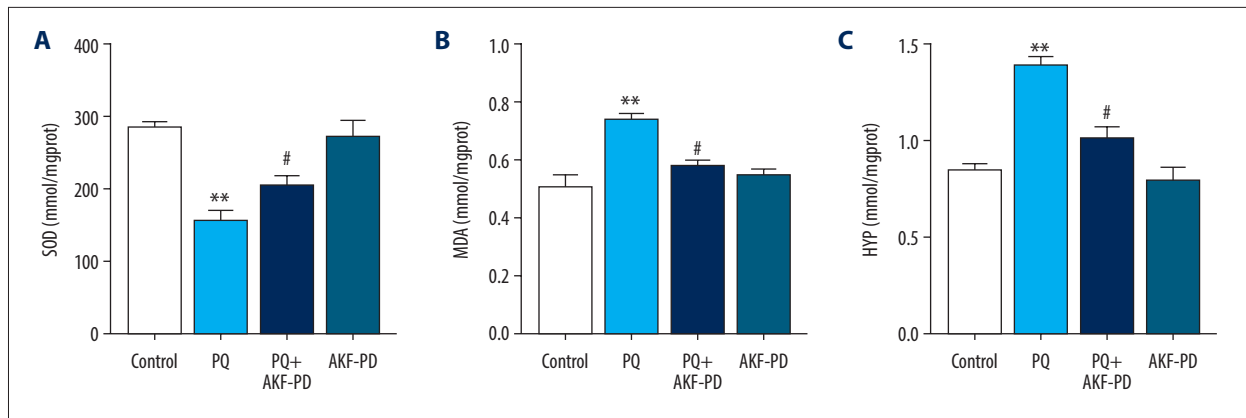


Figure 2. (A-C) Effect of fluorofenidone on SOD, MDA, and HYP levels in lung tissues. Each value represents the mean±SD of 4 independent experiments. ## $P < 0.01$, # $P < 0.05$ vs the model group; ** $P < 0.01$, * $P < 0.05$ vs Controls.

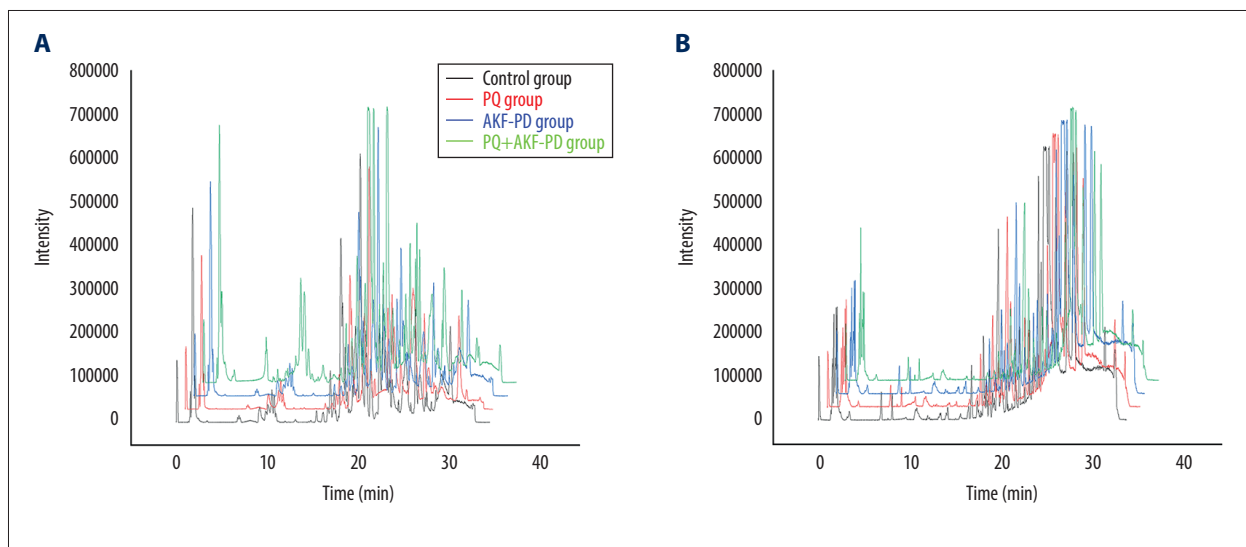


Figure 3. Representative base peak chromatogram (BPC) of serum obtained from different groups of rats in the positive mode (A) and negative mode (B).

Results

Histopathology

Lung tissue sections were observed under a light microscope (Figure 1A), then the degree of alveolitis and pulmonary fibrosis was graded according to Szapiel's semi-quantitative method (Figure 1B). The results showed that the lung tissue in the control group was clear and exhibited no alveolar interval thickening, no inflammation or fibrosis, and no obvious exudation in the alveolar cavity. In the paraquat-exposure group, a large number of inflammatory substances were exuded into the alveolar cavity, the local alveolar structure disappeared, and pulmonary interstitial fibrocyte proliferation occurred. Lung tissue was normal in the group treated with fluorofenidone only and did not differ from tissue in the control group. However, the degree of alveolitis and pulmonary fibrosis in the group exposed

to paraquat and treated with fluorofenidone was significantly lower than that in the paraquat-only group.

Oxidative Stress and Collagen Content

The role of oxidative stress in the development of pulmonary fibrosis has been widely recognized [25]. Paraquat poisoning generates large quantities of oxygen free radicals, causing consumption of superoxide dismutase and subsequently reducing its activity and increasing the levels of the oxidative stress marker malondialdehyde [26]. Hydroxyproline is an indicator of collagen deposition and fibroblast proliferation [27]. Therefore, we measured the levels of malondialdehyde, superoxide dismutase, and hydroxyproline in lung tissue (Figure 2). Superoxide dismutase levels were significantly lower in the paraquat group than in the control group ($P < 0.01$), while malondialdehyde and hydroxyproline levels were higher

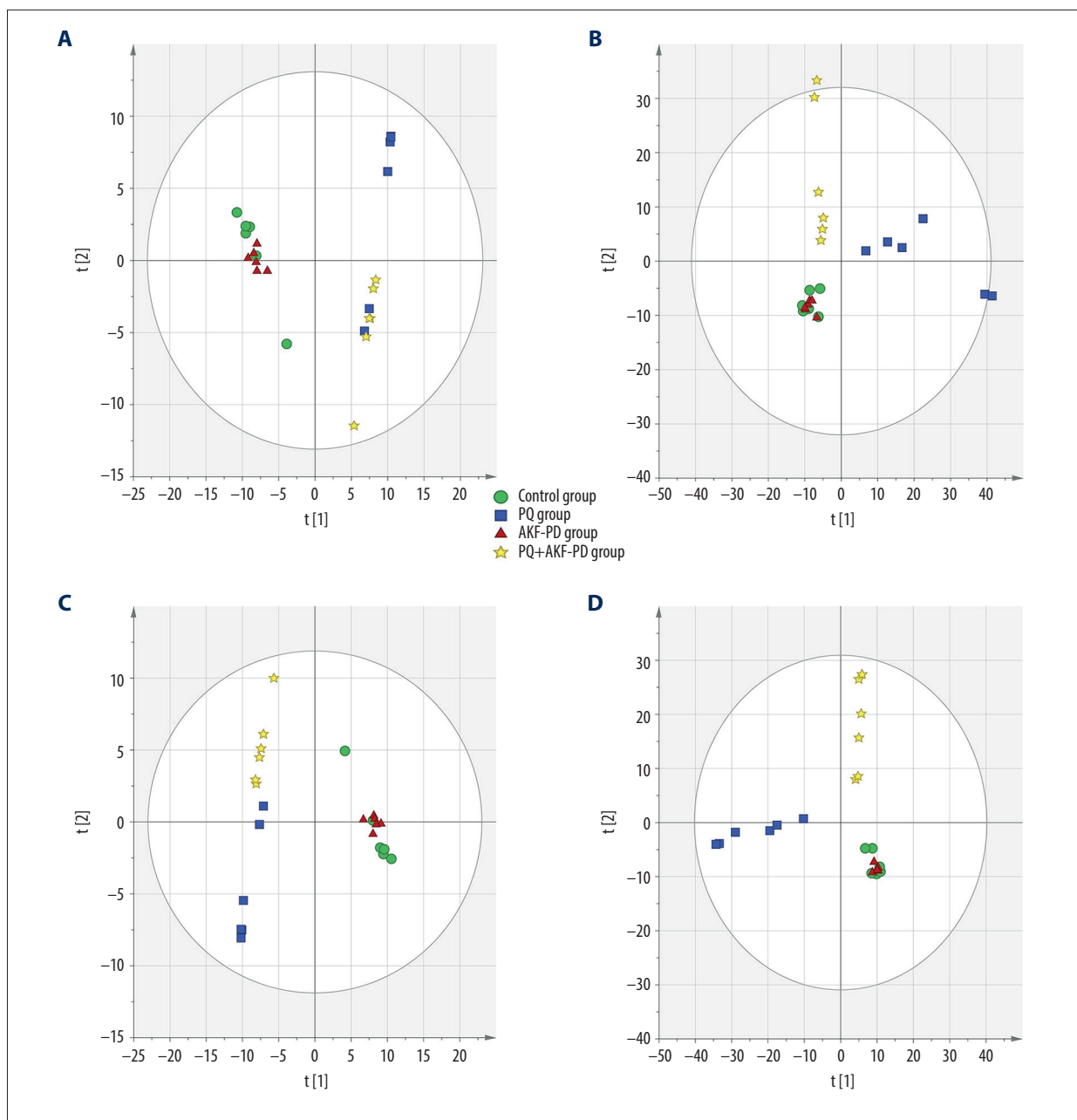


Figure 4. The PCA plot of samples in positive ion mode (A) and in negative ion mode (B). The PLS-DA plot of samples in positive ion mode (C) and in negative ion mode (D).

($P < 0.05$). However, superoxide dismutase levels were significantly higher in the group exposed to paraquat and treated with fluorofenidone than in the paraquat-only group ($P < 0.01$), while malondialdehyde and hydroxyproline levels were lower ($P < 0.01$), indicating that fluorofenidone is effective in treating paraquat-induced pulmonary fibrosis.

Metabolic Spectrum Analysis of Representative Samples

Representative samples were analyzed by UPLC-QTOF-MS metabolic spectrum. As shown in Figure 3, no abnormality was found in the total ion chromatogram, and the reproducibility of sample retention time and the stability of the system were good.

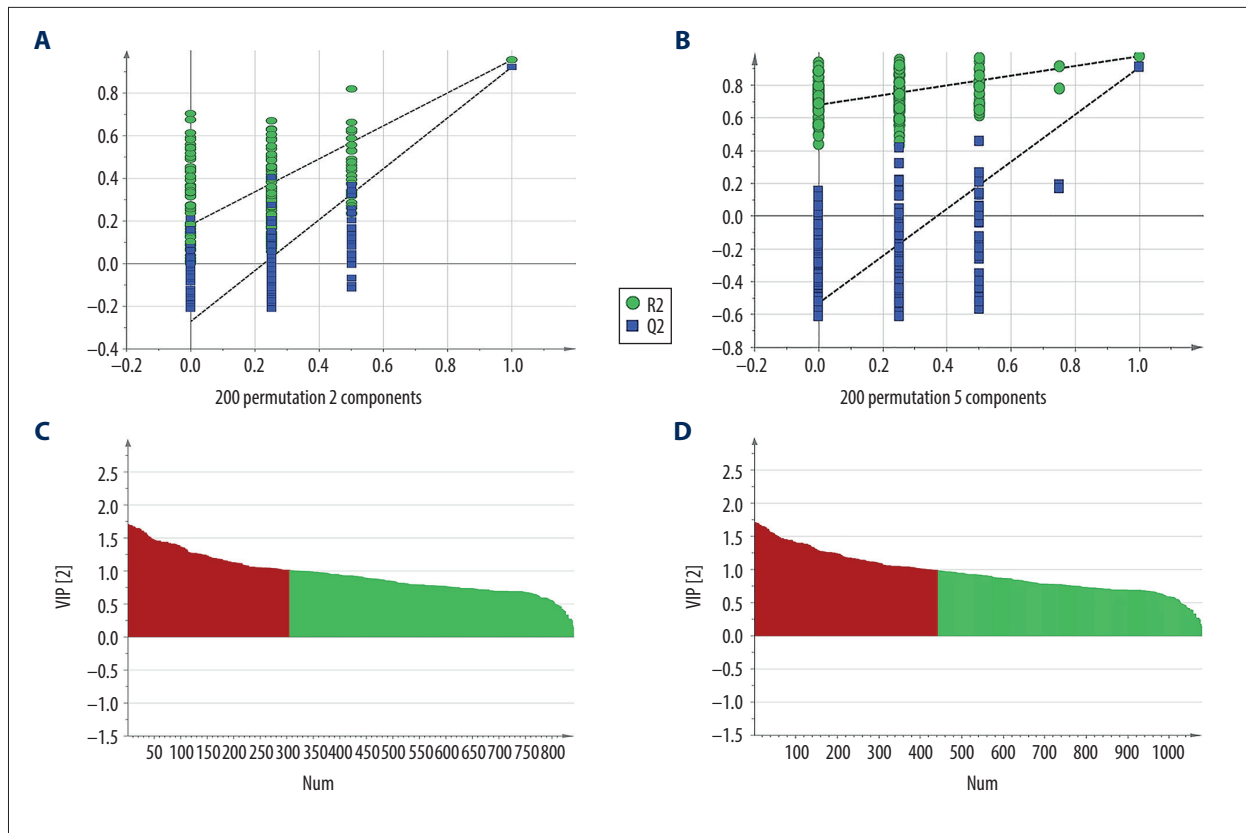


Figure 5. The permutation test of the 4 groups in positive ion mode (A) and in the negative mode (B); the VIP plot of the 4 groups in positive ion mode (C) and in the negative mode (D).

Screening and Identification of Potential Biomarkers

Each sample yielded 2 datasets established by positive and negative ion mode. After normalization and centering, the ion peak areas of the experimental groups were then analyzed by SIMCA-P for principal components. **Figure 4A and 4B** shows that the dividing line between the 4 groups was unclear. To observe differences between groups more intuitively, we conducted a supervised partial least-squares discriminant analysis of the data (**Figure 4C, 4D**). The 4 groups then appeared separated, indicating differences in metabolic responses. Additionally, a permutation of 200 was used to validate the partial least-squares discriminant analysis model and exhibited good results without overfitting (**Figure 5**). The variable importance plot reflects the influence of each variable on the classification and interpretability of each sample group. It is generally accepted that a variable importance plot value greater than 1 indicates that the variable contributes significantly to the separation between groups [28]. In this study, we used a variable importance plot value >1.0 to screen potentially differential compounds. The levels of 18 metabolites differed significantly between samples from the control and paraquat groups ($P < 0.05$, **Table 1**). Thirteen of these metabolites (oleic acid, linoleic acid, 11Z-eicosenoic acid, retinal, retinyl

ester, L-cysteine, glutathione, L-kynurenine, tryptophanamide, arginine, D-galactose, 6-phosphogluconic acid, and citric acid) were modulated by fluorofenidone treatment.

Metabolite Analysis

We used MetaboAnalyst software to analyze the pathways of differentially expressed endogenous metabolites (**Figure 6A**). Pathways identified were those related to the metabolism of linoleic acid, retinol, glutathione, amino acids, and energy (**Figure 6B**).

Network Pharmacology Analysis

According to the 3D chemical structure (**Figure 7A**), we obtained 12 potential targets related to the treatment of pulmonary fibrosis with fluorofenidone through screening of pharmacophores. We visualized the “drug-target-disease” relationship through Cytoscape 3.7.0 software, and obtain the network relationship between fluorofenidone, pulmonary fibrosis, and targets (**Figure 7B**). The red diamond represents pulmonary fibrosis, the green circle represents fluorofenidone, the purple triangle represents the target of the action, and the line represents the relationship between drugs, diseases, and targets.

Table 1. Identification of significantly different metabolites from control, PQ, and PQ+AKF-PD groups by UPLC-QTOF-MS.

No	m/z	Metabolite	Formula	VIP	Fold change (control/PQ)	Fold change (PQ+AKF-PD/PQ)	Pathway involved
1	134.09	Malic acid	C ₄ H ₆ O ₅	1.13074	2.5447↑*	1.6942↓*	Amino sugar and nucleotide sugar metabolism
2	208.21	L-Kynurenine	C ₁₀ H ₁₂ N ₂ O ₃	1.11808	1.41978↑*	0.61965↑*	Tyrosine metabolism
3	307.33	Glutathione	C ₁₀ H ₁₇ N ₃ O ₆ S	1.03463	0.0584↓*	2.2952↑*	Glutathione metabolism
4	495.33	LysoPC160	C ₂₅ H ₅₀ NO ₇ P	1.18742	1.8909↑*	1.5564↑*	Glycerophospholipid metabolism
5	250.29	Ubiquinone-1	C ₁₄ H ₁₈ O ₄	1.14904	1.8712↑*	1.8611↑*	
6	282.5	Oleic acid	C ₁₈ H ₃₄ O ₂	1.18412	1.5532↑*	0.48813↓*	Biosynthesis of unsaturated fatty acids
7	95.979	Phosphoric acid	HO ₄ P-2	1.09284	0.5675↓*	0.82607↓*	
8	284.4	Retinal	C ₂₀ H ₂₈ O	1.17126	0.5198↓*	1.5389↑*	Retinol metabolism
9	276.14	6-Phosphogluconic acid	C ₆ H ₁₃ O ₁₀ P	1.64293	1.514↓*	0.2113↓*	Pentose phosphate pathway
10	204.22	Tryptophan	C ₁₁ H ₁₂ N ₂ O ₂	1.34319	0.1111↓*	1.3933↑*	Tryptophan metabolism
11	310.5	11Z-Eicosenoic acid	C ₂₀ H ₃₈ O ₂	1.40242	0.1408↓*	1.3846↑*	Biosynthesis of unsaturated fatty acids
12	302.5	Retinyl ester	C ₂₀ H ₃₀ O ₂	1.17126	0.359↓*	1.2502↓*	Retinol metabolism
13	280.4	Linoleic acid	C ₁₈ H ₃₂ O ₂	1.31638	0.2517↓*	1.97377↑*	Linoleic acid metabolism
14	476.6	Retinoyl b-glucuronide	C ₂₆ H ₃₆ O ₈	1.17126	0.2505↓*	0.0379↓*	Retinol metabolism
15	180.16	D-Galactose	C ₆ H ₁₂ O ₆	1.09284	1.2251↑*	0.97158↓*	Galactose metabolism
16	130.1	Citraconic acid	C ₅ H ₆ O ₄	1.0432	1.135↓*	0.937↓*	Tricarboxylic acid cycle
17	178.21	Cysteinylglycine	C ₅ H ₁₀ N ₂ O ₃ S	1.47294	0.96835↓*	1.01868↑*	Cysteine and methionine metabolism
18	188.23	Homo-L-arginine	C ₇ H ₁₆ N ₄ O ₂	1.44482	1.0304↑*	0.7317↓*	Arginine metabolism

* The values were statistically significant ($p < 0.05$); ↑ The metabolites were up-regulated; ↓ The metabolites were down-regulated.

The results show that fluorofenidone has the characteristics of multi-target effects in the treatment of pulmonary fibrosis.

The GO analysis results show that there are 14 biological processes ($P < 0.05$), mainly involving proteoglycan binding, collagen binding, 1-phosphatidylinositol-3-kinase activity, phosphatidylinositol 3-kinase activity, insulin receptor substrate binding, phosphatidylinositol phosphate kinase activity, phosphatidylinositol kinase activity, and other enzyme activities (Figure 8). The results reflected that the mechanism of fluorofenidone in the treatment of pulmonary fibrosis may involve the regulation of multiple biological processes.

According to the KEGG enrichment analysis, a total of 103 signal pathways conformed to $P < 0.05$, mainly involving apoptosis,

autophagy, AMPK signaling pathway, type II diabetes mellitus, regulation of lipolysis in adipocytes, and other signal pathways (Figure 9). According to the P value, 20 major signaling pathways were screened, of which apoptosis and autophagy were observed to have the lowest P value of 5.83×10^{-5} . It is well known that autophagy plays an important role in the development of pulmonary fibrosis, and the reduction of autophagy activity promotes the occurrence of pulmonary fibrosis [29]. Therefore, fluorofenidone was most likely to play an anti-pulmonary fibrosis role by regulating the autophagy signal pathway.

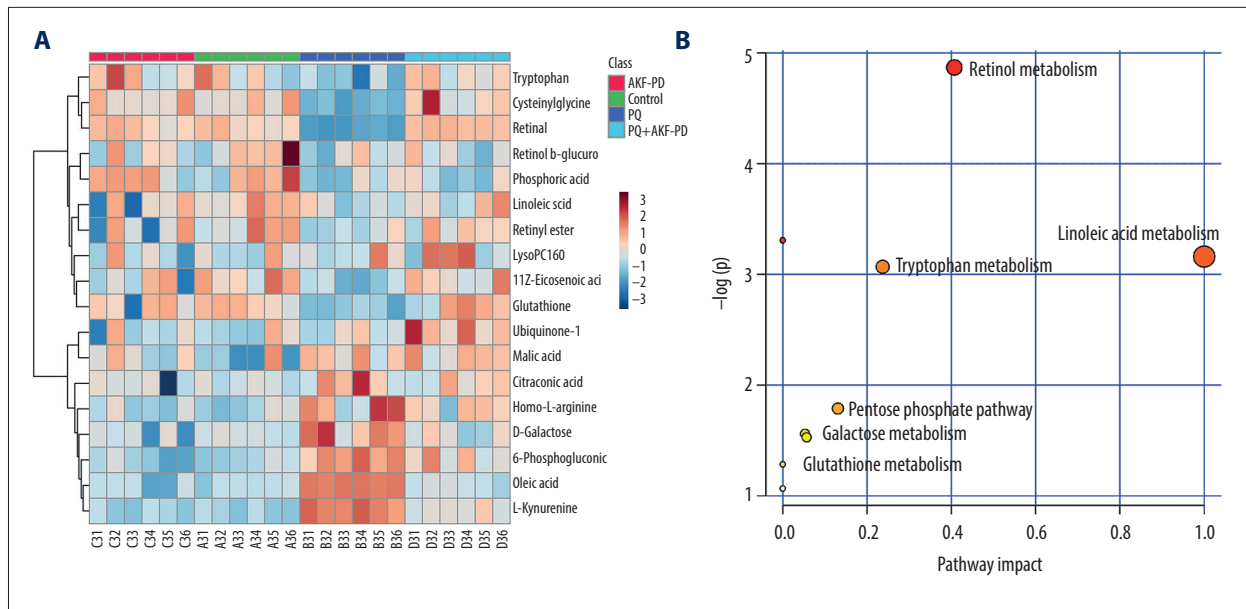


Figure 6. (A) The heat map of the disordered metabolites in different groups. (B) The metabolic pathway map of differential metabolites.

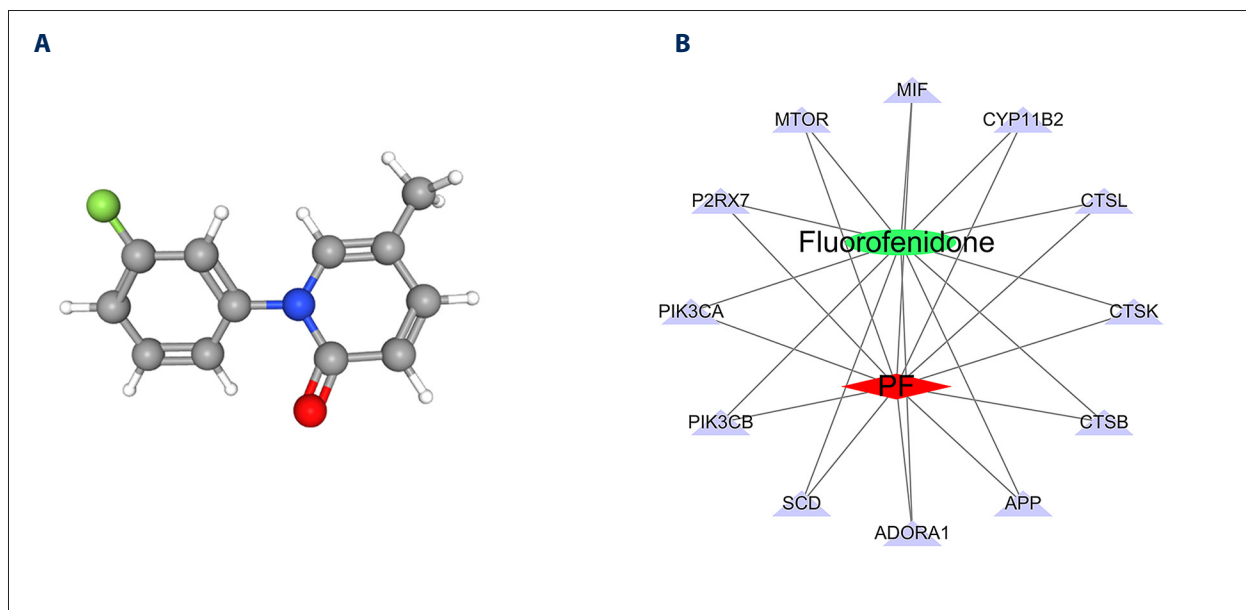


Figure 7. (A) 3D structure of fluorofenidone; (B) The drug-target-disease network. The red diamond represents pulmonary fibrosis, the green circle represents fluorofenidone, the purple triangle represents the target of action, and the line represents the relationship between drugs, diseases, and targets.

Fluorofenidone Attenuates Pulmonary Fibrosis by Upregulating Autophagy

To further verify the effect of fluorofenidone on autophagy, we detected the expression of autophagy-related proteins LC3-II/I and p62 by western blotting. The results are shown in **Figure 10A**. In the PQ group, LC3-II/I decreased significantly, and p62 increased ($P < 0.05$). However, after treatment with

fluorofenidone, the expression of LC3-II/I increased significantly, and the expression of p62 decreased ($P < 0.05$). To determine whether autophagy was involved in the anti-pulmonary fibrosis effects of fluorofenidone, the expression of pulmonary fibrosis-related proteins α -SMA, TGF- β 1, and E-cadherin were detected. The results of western blot analysis revealed that the expression levels of α -SMA and TGF- β 1 were significantly higher in the paraquat group than in the control group, and

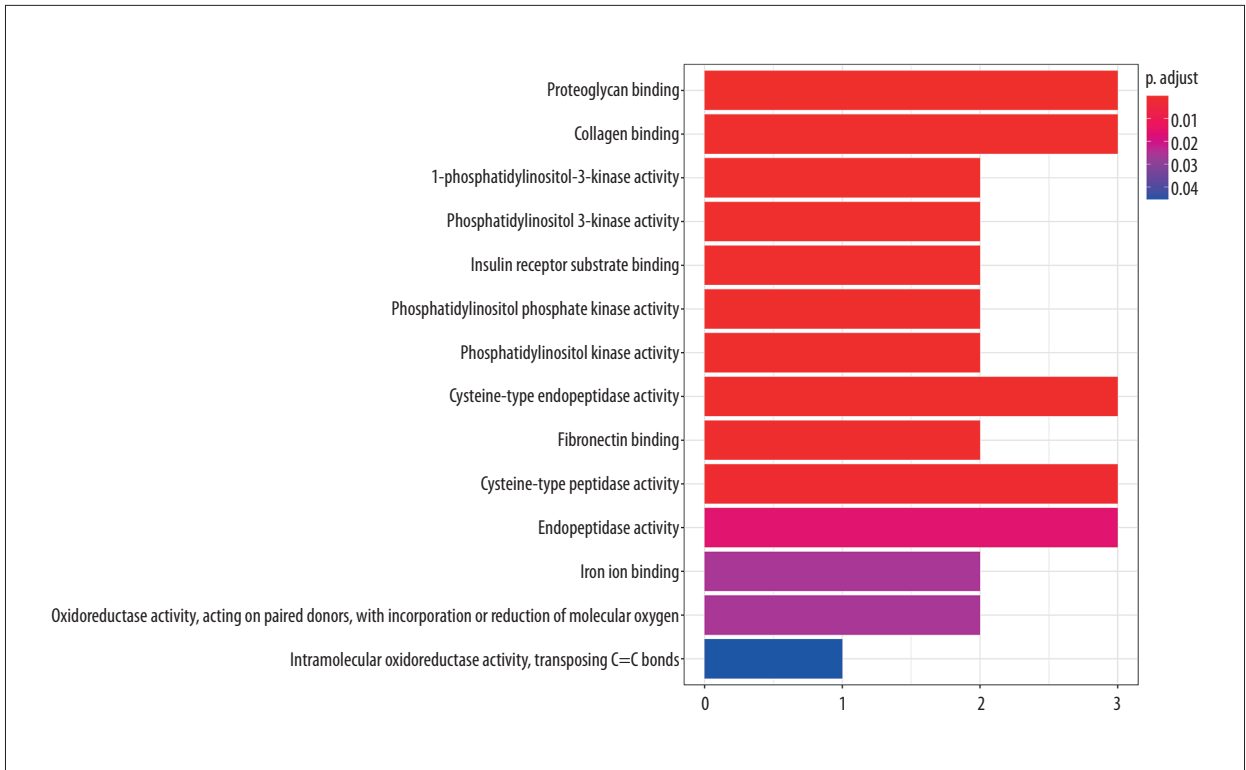


Figure 8. GO function enrichment analysis.

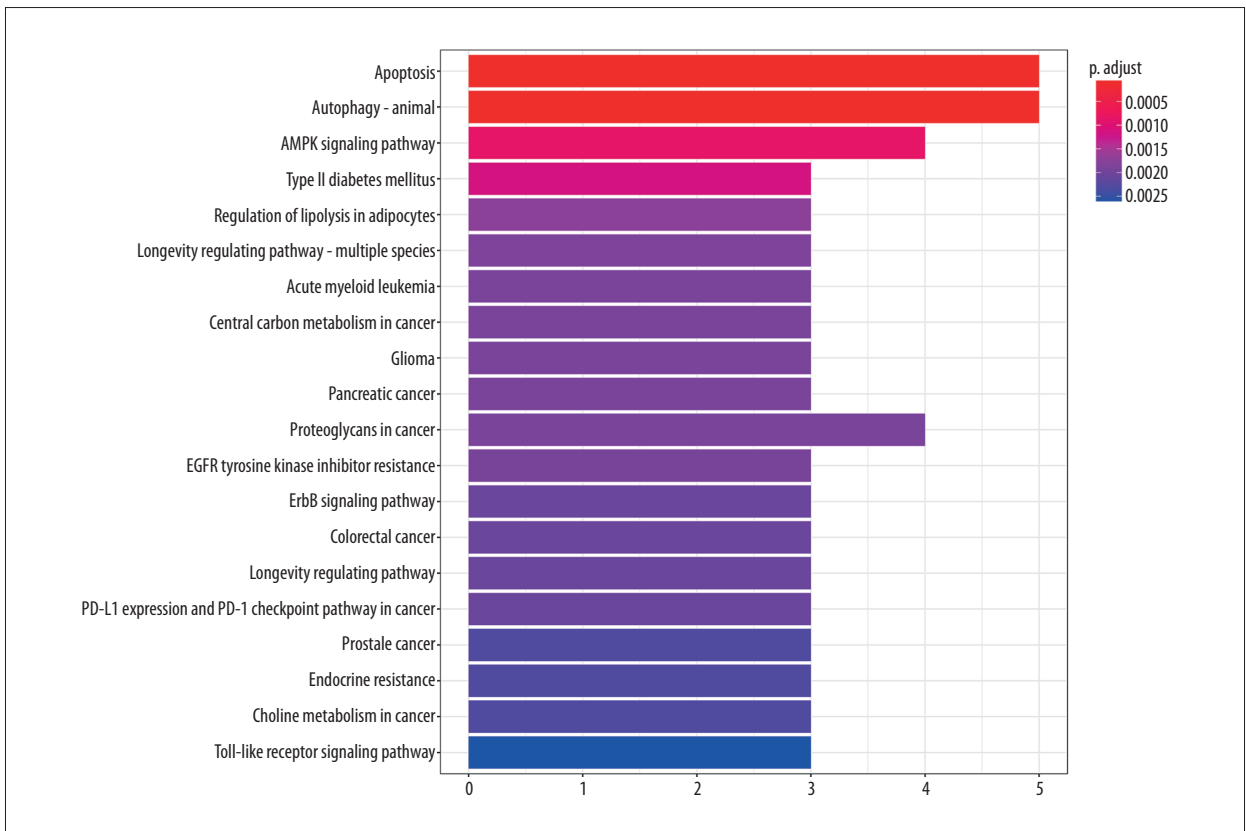


Figure 9. KEGG signal path enrichment analysis (top 20).

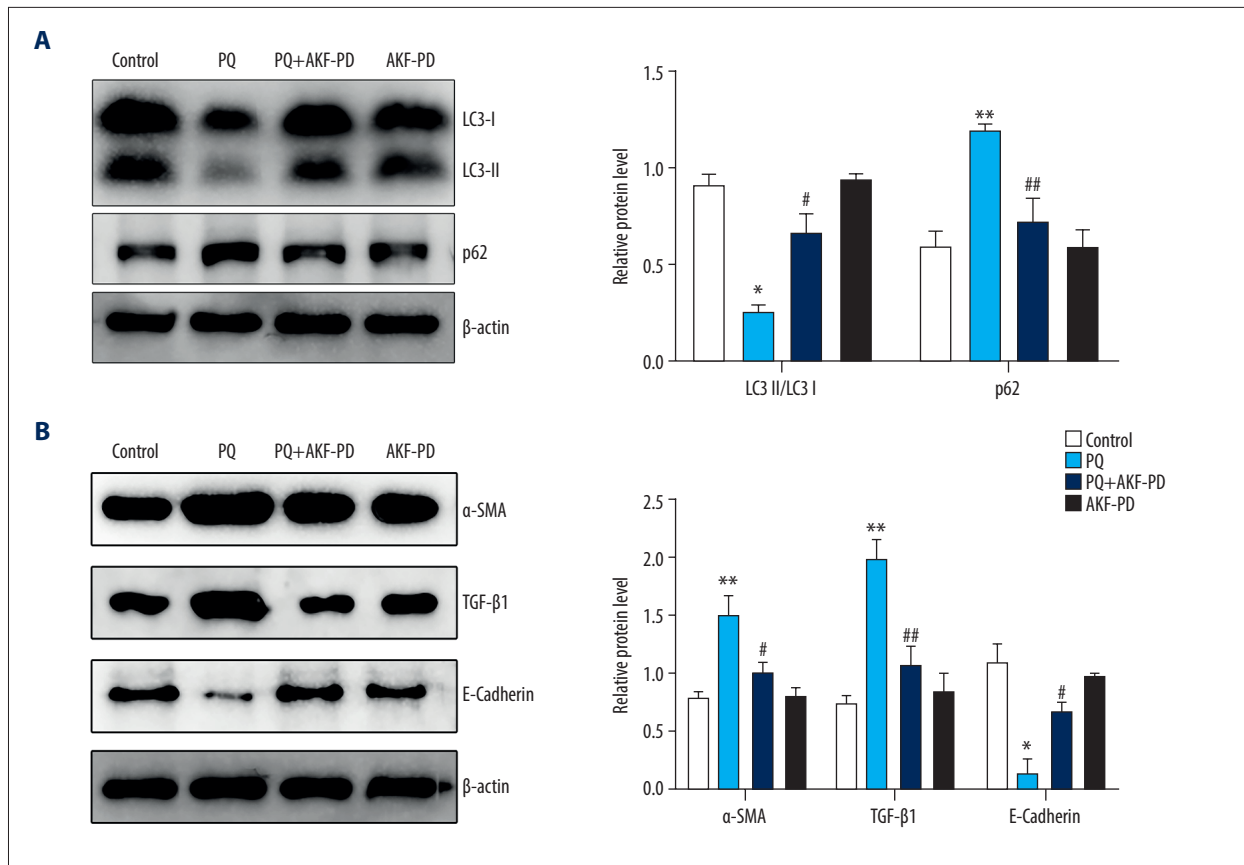


Figure 10. Fluorofenidone attenuated pulmonary fibrosis by upregulating autophagy. (A), Effects of fluorofenidone on the expression of fibrosis-related proteins in rat lung tissue. (B), Effects of fluorofenidone on the expression of autophagy-related proteins in rat lung tissue. * $P < 0.05$ vs the control group; ** $P < 0.01$ vs the control group; # $P < 0.05$ vs the PQ group.

the level of E-cadherin level was lower, while fluorofenidone treatment almost totally abolished paraquat-induced upregulation of α -SMA and TGF- β 1 expressions, and significantly increased the expression levels of E-cadherin (Figure 10B). The results show that fluorofenidone can inhibit the development of paraquat-induced pulmonary fibrosis by increasing autophagy.

Discussion

We used UPLC-QTOF-MS to study the effect of fluorofenidone on plasma metabolites in paraquat-exposed rats, and identified 13 potential biomarkers that may be related to the metabolism of fatty acids, retinol, glutathione, amino acids, and energy. Our findings indicate a therapeutic role for fluorofenidone in restoring functional metabolism.

Oleic acid, linoleic acid, and 11Z-eicosenoic acid are unsaturated fatty acids, which is a class of compounds that can inhibit various inflammatory mediators and cytokines [30]. The monounsaturated oleic acid is involved in the formation of phospholipids and triglycerides. There is evidence that oleic

acid is toxic when triglyceride synthesis is blocked and can promote the secretion of type I and IV collagen and fibronectin [31,32]. We found higher levels of oleic acid in the plasma of paraquat-exposed rats, suggesting that oleic acid can contribute to the formation of paraquat-induced pulmonary fibrosis. Linoleic acid is a functional polyunsaturated fatty acid that can enhance immunity by increasing the production of non-specific antibodies, the proliferation of lymphocytes, and phagocytic capacity [33]. In this study, we found lower levels of linoleic acid in the plasma of rats exposed to paraquat, which suggests that paraquat affects the expression of immunoglobulins, thereby increasing the release of inflammatory factors. Treatment with fluorofenidone increased linoleic acid levels, supporting the hypothesis that fluorofenidone enhances immunity and alleviates inflammation.

Retinol and retinyl ester are the intermediate metabolites of retinol, which promotes growth and development and can enhance immunity by increasing the infiltration of lymphocytes and alveolar macrophages. Retinol has also been shown to be protective of the alveolar and airway epithelia [34]. Although retinol cannot remove free radicals, it exerts an antioxidant

effect by inhibiting the generation of active oxygen species. Thus, dysregulation of retinol metabolism will have a direct effect on the formation of keratin in thymic epithelial cells, resulting in declines in immune function [35]. Animal experiments have shown that retinol promotes the proliferation and separation of alveolar wall cells, improving damaged alveolar structures, and reducing the degree of emphysema, while retinol deficiency can lead to emphysema [36]. In the present study, paraquat reduced the levels of retinal and retinyl ester in lung tissue, suggesting that paraquat exposure can result in the destruction of airway epithelial integrity and declines in immune function. Fluorofenidone treatment increased the levels of retinal and retinyl esters in lung tissue, and may be protective of airway epithelial cells and immunity.

Glutathione is a tripeptide synthesized from cysteine, glutamic acid, and glycine. It serves as an antioxidant, a regulator of cell proliferation, and an agent of biotransformation, protecting large molecules such as proteins, lipids, and DNA from peroxidative damage [37-39]. Lower glutathione levels affect multiple cellular redox signaling processes, leading to the upregulation of factors related to inflammation and fibrosis, such as tumor necrosis factor α and interleukin 1, 6, and 8. Studies have shown that paraquat-poisoned patients are unable to maintain the oxidation/reduction balance because of glutathione deficiency in the lung [40,41]. Treatment with reduced glutathione can alleviate the symptoms of acute renal injury in paraquat-exposed rats and reduce inflammation by suppressing the expression of nitric oxide synthetase and cyclooxygenase, activation of nuclear factor-kappa B, and the activity of lysosomal protease [42]. In the present study, paraquat exposure reduced glutathione content via oxidative stress but fluorofenidone treatment restored it, suggesting that fluorofenidone can selectively scavenge free radicals to reduce the consumption of glutathione.

Paraquat impairs the metabolism of multiple amino acids. In this study, we found dysregulation in arginine, tryptophan, and L-kynurenine. Arginine can affect cellular immunity under stress conditions [43]. Tryptophan is essential for protein synthesis and some physiological metabolic functions [44]. An immune response generally reduces tryptophan levels in tissues and blood. Furthermore, tryptophan has been shown to reduce serum malondialdehyde and enhance superoxide dismutase activity [45]. L-Kynurenine is an important immune-related metabolite involved in pathological processes such as excitotoxicity, neuroinflammation, oxidative stress, and mitochondrial damage [46,47]. Overall, amino acids are involved in maintaining the energy balance and in regulating oxidative stress and immunity after injury. We found that the therapeutic effect of fluorofenidone was related to its regulation of amino acid metabolism.

Paraquat poisoning can damage multiple organs, although its main target organ is the lungs. The redox reaction interferes with mitochondrial electron transfer, generates a large number of oxygen free radicals, induces lipid peroxidation, and leads to mitochondrial dysfunction and impairment of the tricarboxylic acid (TCA) cycle and respiratory chain transfer [48]. We found that paraquat exposure increased citric acid levels; citric acid is an intermediate product of the TCA cycle, indicating that paraquat poisoning blocks the TCA cycle to affect energy supply [49]. Galactose is a reducing monosaccharide that can be metabolized to glucose under normal conditions, but an excess leads to formation of reactive oxygen species and advanced glycation end-products, which can result in oxidative stress, mitochondrial dysfunction, cell damage, and inflammation [50-52]. Paraquat has been reported to interfere with glucose metabolism and the TCA cycle in dopaminergic neurons [53]. In this study, fluorofenidone treatment restored the levels of products related to the TCA cycle and glucose metabolism pathway (citric acid, 6-phosphogluconic acid, and galactose), indicating that fluorofenidone can regulate energy metabolism.

Network pharmacology explains the development of diseases from the perspective of systems biology and biological network balance, and understands the interaction between drugs and the body from the overall perspective of improving or restoring biological network balance [54]. In addition, it helps to predict the target of the drug in treatment of the disease. Based on the results of metabolomics research, this study found 12 targets related to the treatment of pulmonary fibrosis by fluorofenidone through network pharmacological analysis. The results of the KEGG pathway analysis revealed that fluorofenidone exerts anti-pulmonary fibrosis effects by acting in 20 signaling pathways, among which autophagy had the smallest *P* value, indicating that it was easiest for fluorofenidone to perform its anti-pulmonary fibrosis effect by regulating these pathways. Autophagy is a self-protection mechanism of cells, which plays an important role in regulating cell survival and apoptosis. Studies have shown that autophagy is closely related to pulmonary fibrosis, and insufficient autophagy promotes the occurrence and development of pulmonary fibrosis [55,56]. In this study, western blot analysis was performed to further confirm that fluorofenidone can alleviate pulmonary fibrosis by regulating autophagy. The results showed that pretreatment with fluorofenidone upregulated the expression of LC3II/I and E-cadherin, and downregulated the expression of p62, α -SMA, and TGF- β 1, which validated that fluorofenidone inhibited the development of paraquat-induced pulmonary fibrosis by increasing autophagy.

Conclusions

The present study combined metabolomics and network pharmacology analysis to investigate the mechanism of paraquat-induced pulmonary fibrosis and revealed the efficiency and possible mechanisms of fluorofenidone in the treatment of pulmonary fibrosis. Pathology study results showed a significant improvement after fluorofenidone treatment. In a UPLC-QTOF-MS-based non-targeted metabolomics study, a total of 13 significantly altered biomarkers in rat serum were identified and shown to be involved in the tryptophan metabolism, glutathione metabolism, biosynthesis of unsaturated fatty acids, retinol metabolism, pentose phosphate pathway, linoleic acid metabolism, galactose metabolism, and TCA cycle. The network pharmacology analysis screened 12 targets, and found multiple signaling pathways and metabolic pathways

that exert anti-pulmonary fibrosis effects. Furthermore, the results of western blot analysis validated that fluorofenidone can alleviate the development of pulmonary fibrosis by increasing autophagy. Our results provide the basis for further studies to fully elucidate the anti-pulmonary fibrosis effects of fluorofenidone.

Acknowledgements

We thank Liwen Bianji, Edanz Group China (<https://en-author-services.edanzgroup.com/ac>), for editing the English text of a draft of this manuscript.

Conflicts of Interest

None.

References:

1. He F, Zhou A, Feng S, et al. Mesenchymal stem cell therapy for paraquat poisoning: A systematic review and meta-analysis of preclinical studies. *PLoS One*, 2018;13(3):e0194748
2. Zhang H, You L, Zhao M. Rosiglitazone attenuates paraquat-induced lung fibrosis in rats in a PPAR gamma-dependent manner. *Eur J Pharm*, 2019;851:133-43
3. Rasooli R, Pourgholamhosein F, Kamali Y, et al. Combination therapy with pirfenidone plus prednisolone ameliorates paraquat-induced pulmonary fibrosis. *Inflammation*, 2018;41(1):134-42
4. Wijsenbeek M. Progress in the treatment of pulmonary fibrosis. *Lancet Respir Med*, 2020;8(5):424-25
5. Kropski JA, Blackwell TS. Progress in understanding and treating idiopathic pulmonary fibrosis. *Ann Rev Med*, 2019;70(1):211-24
6. Aggarwal S, Mannam P, Zhang J. Differential regulation of autophagy and mitophagy in pulmonary diseases. *Am J Physiol Lung Cell Mol Physiol*, 2016;311(2):L433-52
7. Dewage SNV, Organ L, Koumoundouros E, et al. The efficacy of pirfenidone in a sheep model of pulmonary fibrosis. *Exp Lung Res*, 2019;45(22): 1-13
8. Fois AG, Posadino AM, Giordo R, et al. Antioxidant activity mediates pirfenidone antifibrotic effects in human pulmonary vascular smooth muscle cells exposed to sera of idiopathic pulmonary fibrosis patients. *Oxid Med Cell Longev*, 2018;2018:2639081
9. Pourgholamhosein F, Rasooli R, Pourmamdari M, et al. Pirfenidone protects against paraquat-induced lung injury and fibrosis in mice by modulation of inflammation, oxidative stress, and gene expression. *Food Chem Toxicol*, 2017;112:39-46
10. Wu JP, He LY, Yun JJ, et al. Confirmation and quality control of a photopolymerized substance in fluorofenidone. *J Pharm Anal*, 2012;43(2):159-63
11. Yang H, Zhang W, Xie T, et al. Fluorofenidone inhibits apoptosis of renal tubular epithelial cells in rats with renal interstitial fibrosis. *Braz J Med Biol Res*, 2019;52(11):e8772
12. Chen H, Gan Q, Yang C, et al. A novel role of glutathione S-transferase A3 in inhibiting hepatic stellate cell activation and rat hepatic fibrosis. *J Transl Med*, 2019;17(1):280
13. Chen LX, Yang K, Sun M, et al. Fluorofenidone inhibits transforming growth factor- β 1-induced cardiac myofibroblast differentiation. *Die Pharmazie*, 2012;67(5):452-56
14. Yang H, Zhang W, Xie T, et al. Fluorofenidone inhibits apoptosis of renal tubular epithelial cells in rats with renal interstitial fibrosis. *Braz J Med Biol Res*, 2019;52(11):e8772
15. Song C, He L, Zhang J, et al. Fluorofenidone attenuates pulmonary inflammation and fibrosis via inhibiting the activation of NALP3 inflammasome and IL-1/IL-1R1/MyD88/NF- κ B pathway. *J Cell Mol Med*. 2016;20(11):2064-77
16. Li L, Luo X, Cheng Z. In vitro inhibition and induction of human liver cytochrome P450 enzymes by a novel anti-fibrotic drug fluorofenidone. *Xenobiotica*, 2020 [Online ahead of print]
17. Liu J, Song C, Xiao Q, et al. Fluorofenidone attenuates TGF- β 1 – induced lung fibroblast activation via restoring the expression of Caveolin-1. *Shock*, 2015;43(2):201-7
18. Jing, Tang, Jianming, et al. Spermidine-mediated poly(lactic-co-glycolic acid) nanoparticles containing fluorofenidone for the treatment of idiopathic pulmonary fibrosis. *Int J Nanomedicine*, 2017;12:6687-704
19. Wu YH, Li XW, Li WQ, et al. Fluorofenidone attenuates bleomycin-induced pulmonary fibrosis by inhibiting eukaryotic translation initiation factor 3a (eIF3a) in rats. *Eur J Pharmacol*, 2016;773:42-50
20. Gao X, Zhang W, Wang Y, et al. Serum metabolic biomarkers distinguish metabolically healthy peripherally obese from unhealthy centrally obese individuals. *Nutr Metab*, 2016; 13(1):1-10
21. Shi J, Cao B, Wang XW, et al. Metabolomics and its application to the evaluation of the efficacy and toxicity of traditional Chinese herb medicines. *J Chromatogr B*, 2016;1026:204-16
22. Duan C, Li Y, Dong X, et al. Network pharmacology and reverse molecular docking-based prediction of the molecular targets and pathways for avicularin against cancer. *Comb Chem High Throughput Screen*, 2019;22(1):4-12
23. Tan W, Wang W, Zheng X, et al. [Effect of fluorofenidone on renal interstitial fibrosis in rats with unilateral ureteral obstruction.] *Zhong Nan Da Xue Xue Bao Yi Xue Ban*, 2018;43(5):511-19 [in Chinese]
24. Szapiel SV, Elson NA, Fulmer JD, et al. Bleomycin-induced interstitial pulmonary disease in the nude, athymic mouse. *Am Rev Respir Dis*, 1979;120(4):893-99
25. Otoupalova E, Smith S, Cheng G, et al. Oxidative stress in pulmonary fibrosis. *Compr Physiol*. 2020;10(2):509-47
26. Zhenhua L, Xuedong K, Kunpeng Z, et al. Effect of Shaoyin kidney supporting and pivot adjusting method on serum SOD, MDA, GSH-PX in STZ-induced diabetic rats. *East Asian Sci Technol Med*, 2018
27. Zhang L, Li Q, Liu W, et al. Mesenchymal stem cells alleviate acute lung injury and inflammatory responses induced by paraquat poisoning. *Med Sci Monit*, 2019;25:2623-32
28. Zhang G, Wang H, Xie W, et al. Comparison of triterpene compounds of four botanical parts from *Poria cocos* (Schw.) wolf using simultaneous qualitative and quantitative method and metabolomics approach. *Food Res Int*, 2019;121:666-77
29. Im J, Hergert P, Nho RS. Reduced FoxO3a expression causes low autophagy in idiopathic pulmonary fibrosis fibroblasts on collagen matrices. *Am J Physiol Lung Cell Mol Physiol*, 2015;309(6):L552-61

30. Wu J, Chu Z, Ruan Z, et al. Changes of intracellular porphyrin, reactive oxygen species, and fatty acids profiles during inactivation of methicillin-resistant *Staphylococcus aureus* by antimicrobial blue light. *Front Physiol*, 2018;9:1658
31. Newberry EP, Xie Y, Kennedy SM, et al. Prevention of hepatic fibrosis with liver microsomal triglyceride transfer protein deletion in liver fatty acid binding protein null mice. *Hepatology*, 2017 65(3):836-52
32. Fang S, Cai Y, Lyu F, et al. Exendin-4 improves diabetic kidney disease in C57BL/6 mice independent of brown adipose tissue activation. *J Diabetes Res*, 2020;2020:1-12
33. Huan YS, Li ZD, Ron H, et al. Effects of conjugated linoleic acid on growth, body composition, antioxidant status, lipid metabolism and immunity parameters of juvenile Chu's croaker, *Nibea coibor*. *Aquac Res*, 2018;49(1):13486
34. Ng-Blichfeldt JP, Schrik A, Kortekaas RK, et al. Retinoic acid signaling balances adult distal lung epithelial progenitor cell growth and differentiation. *EBioMedicine*, 2018;36:461-74
35. Timoneda J, Rodríguez-Fernández L, Zaragoza R, et al. Vitamin A deficiency and the lung. *Nutrients*, 2018;10(9):1132
36. Ali MOI, Atia NE, Islam T, et al. Effect of vitamin A on lung function test in patient with chronic bronchial asthma. *TAJ Journal of Teachers Association*, 2018;27(1):10
37. Xalxo R, Keshavkant S. Melatonin, glutathione and thiourea attenuates lead and acid rain-induced deleterious responses by regulating gene expression of antioxidants in *Trigonella foenum graecum* L. *Chemosphere*, 2019; 221:1-10
38. Hussain M, Mahmud A, Hussain J, et al. Effect of dietary amino acid regimens on growth performance and body conformation and immune responses in Aseel chicken. *Indian Journal of Animal Research*, 2018; ijar.B-767
39. Li T, Yu B, Liu Z, et al. Homocysteine directly interacts and activates the angiotensin II type I receptor to aggravate vascular injury. *Nat Commun*, 2018;9(1):11
40. Zhang S, Hu R Li H. Glutathione modified Ag nanoparticles as efficient detector for pyrimethanil. *Nanotechnology*, 2019;30(11):115502
41. Admoni SN, Santos-Bezerra DP, Perez RV, et al. Glutathione peroxidase 4 functional variant rs713041 modulates the risk for cardiovascular autonomic neuropathy in individuals with type 1 diabetes. *Diab Vasc Dis Res*, 2019;16(3):297-99
42. Rao GN, Sadasivudu B, Cotlier E. Studies on glutathione S-transferase, glutathione peroxidase and glutathione reductase in human normal and cataractous lenses. *Ophthalmic Res*, 2017;15(4):173-79
43. Vianna RA, Chideroli R, Costa ARD, et al. Effect of experimental arginine supplementation on the growth, immunity, and resistance of tilapia fingerlings to *Streptococcus agalactiae*. *Aquac Res*, 2020;51(13):1276-83
44. Cao Y, Shen M, Jiang Y, et al. Melatonin reduces oxidative damage in mouse granulosa cells via restraining JNK-dependent autophagy. *Reproduction*, 2018;155(3):307-19
45. Li G, Ma Y, Ji J, et al. Effects of gastrodin on 5-HT and neurotrophic factor in the treatment of patients with post-stroke depression. *Exp Ther Med*, 2018;16(6):4493-98
46. Borisova MA, Snytnikova OA, Litvinova EA, et al. Fucose ameliorates tryptophan metabolism and behavioral abnormalities in a mouse model of chronic colitis. *Nutrients*, 2020;12(2):445
47. Garcez ML, Jacobs KR, Guillemin GJ: Microbiota alterations in Alzheimer's disease: Involvement of the kynurenine pathway and inflammation. *Neurotox Res*, 2019;36(Suppl.1):424-36
48. Maget A, Platzer M, Bengesser SA, et al. Differences in kynurenine metabolism during depressive, manic, and euthymic phases of bipolar affective disorder. *Curr Top Med Chem*, 2019;19(15):1344-52
49. Gafson AR, Savva C, Thorne T, et al. Breaking the cycle: Reversal of flux in the tricarboxylic acid cycle by dimethyl fumarate. *Neurol Neuroimmunol Neuroinflamm*, 2019;6(3):e562
50. Anandhan A, Lei S, Levytskyy R, et al. Glucose metabolism and AMPK signaling regulate dopaminergic cell death induced by gene (α -synuclein)-environment (paraquat) interactions. *Mol Neurobiol*, 2017;54(5):3825-42
51. Cheng SM, Ho YJ, Yu SHz et al. Anti-apoptotic effects of diosgenin in D-galactose-induced aging brain. *Am J Chin Med*, 2020;48(2) 1-16
52. He S, Hu Q, Xu X, et al. Advanced glycation end products enhance M1 macrophage polarization by activating the MAPK pathway. *Biochem Biophys Res Commun*, 2020;525(2):334-40
53. Yuan G, Si G, Hou Q, et al. Advanced glycation end products induce proliferation and migration of human aortic smooth muscle cells through PI3K/AKT pathway. *Biomed Res Int*, 2020;2020(10):1-11
54. Chandran U, Mehendale N, Patil S, et al. Network pharmacology. *Innovative Approaches in Drug Discovery*, 2017;127-64
55. Patel AS, Lin L, Geyer A, et al. Autophagy in idiopathic pulmonary fibrosis. *Int J Basic Clin Pharmacol*, 2014;3(7):e41394
56. Zhao H, Wang Y, Qiu T, et al. Autophagy, an important therapeutic target for pulmonary fibrosis diseases. *Clinica Chimica Acta*, 2019;502:139-47